Quantum Lithography with Classical Light

P. R. Hemmer,[1] A. Muthukrishnan,[2] M. O. Scully,[2,3] and M. S. Zubairy[2]

[1]*Electrical Engineering Department, Texas A&M University, College Station, Texas 77843, USA*
[2]*Institute for Quantum Studies and Department of Physics, Texas A&M University, College Station, Texas 77843, USA*
[3]*Princeton Materials Institute and Department of Mechanical and Aerospace Engineering, Princeton University, Princeton, New Jersey 08544, USA*

(Received 6 June 2005; revised manuscript received 23 February 2006; published 28 April 2006)

We show how to achieve subwavelength diffraction and imaging with classical light, previously thought to require quantum fields. By correlating wave vector and frequency in a narrow band, multiphoton detection process that uses Doppleron-type resonances, we show how to achieve arbitrary focal and image plane patterning with classical laser light at submultiples of the Rayleigh limit, with high efficiency, visibility, and spatial coherence. A frequency-selective measurement process thus allows one to simulate, semiclassically, the path-number correlations that distinguish a quantum entangled field.

DOI: 10.1103/PhysRevLett.96.163603 PACS numbers: 42.50.St, 42.50.Hz, 85.40.Hp

In this Letter, our aim is to examine the role of multiphoton resonant, narrow band measurements on the spatial resolution limits of classical, monochromatic light interference. A fundamental limit to optical resolution arises from the wave nature of light. This is captured by the Rayleigh criterion [1], which limits the feature size of interfering beams to half the wavelength of light. It is interesting to inquire whether the quantum mechanical absorption process underlying multiphoton phenomena leads to ways around the diffraction limit of classical optics. This focuses attention on the measurement process itself, *vis-à-vis* the recording of a particular interference pattern, such as in lithography, as the key to understanding the interferometric properties of light.

Quantum entanglement between photons is recognized to produce novel interference effects in correlation measurements. The wave-particle duality of light is connected with which-path knowledge as encapsulated in the quantum eraser [2]. Specifically, *path-number* entanglement, where photons in different paths (or polarizations) are correlated in photon number, leads to subwavelength fringes that can be useful for microscopy [3,4], lithography [5,6], and magnetometry [7], and, when combined with frequency correlations, leads to subnatural linewidths in spectroscopy [8].

Our purpose is to inquire which, if any, of these remarkable phenomena attributed to entangled photons can be realized using classical light. We focus attention on quantum field lithography [5,6]. Indeed, the difficulty of generating pure, high-order entangled Fock states, plus their selective weak field detection, has recently spurred alternative efforts, such as the use of classical, coherent [9,10], and thermal [11] light to emulate the quantum resolution. In the coherent schemes, the requisite nonlinearity is effectively in the substrate (as in our case), and is accessed through phase delays introduced in the interfering beams, which has the effect of limiting the visibility and/or spatial coherence of the recorded pattern. In the thermal scheme, the correlation of wave vectors is measured at two different detection points, which limits the application to lithography. We show below that with the proper multiphoton detector we can overcome the above limitations, and achieve arbitrary spatial patterning at subwavelength scales using laser light.

Multiphoton phenomena, first discussed by Göppert-Mayer in 1931 [12], have played a key role in both fundamental science and technology. The Hanbury-Brown–Twiss effect in stellar interferometry [13], recognized to be the harbinger of modern quantum optics, showed that two-photon correlations, even of classical light, can have new and interesting imaging properties that go beyond single photon, or linear intensity, measurements. This called for a reevaluation of optical coherence effects in light of a quantum theory of photodetection.

As elucidated by Glauber [14], photodetection is a space-time event corresponding to a pointlike, broadband detector carrying out an absorptive measurement on the field. The paradigm of an ideal photodetector is an atom with a broad final density of states. In practice, however, one usually needs to account for finite bandwidths in the detection process. Mollow [15] considered the implications of a narrow band detector for the quantum field. He showed that the counting rates for two-photon absorption are different for chaotic and laser light depending on the detector bandwidth. Significantly, considerations about the atomic level structure and transition matrix elements now become relevant. The effects of detector bandwidth have also been studied for the case of polychromatic light [16], with respect to the issues of photon flux counting and photoelectric fluctuations.

In our approach to subwavelength interference (see Fig. 1), the basic principle is a correlation of wave vector and frequency such that a narrowband, multiphoton detector absorbs ''bunches'' of photons from different propagation directions. As this is based purely on energy constraints, it can be formulated in the language of photo-

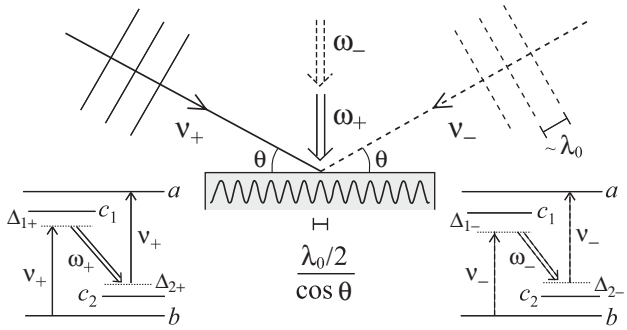

FIG. 1. Subwavelength interference with classical light. Two counterpropagating plane waves consisting of signal frequencies $\nu_\pm$ interfere on a photosensitive substrate. The drive fields $\omega_\pm$ assist a directional resonance for pairs of signal photons. Sinusoidal N-photon interference can be obtained using a frequency multiplet along each direction (c.f. Fig. 2).

detection theory applied to finite bandwidths. The key result is that the direction selectivity of the absorptive measurement process literally *simulates* path-number correlations between counterpropagating photons, a feature that was previously associated with quantized light fields.

The motivation for this study comes from two points of view. One is the early theoretical suggestion [17–19], and experimental observation [20] of directional multiphoton resonances, called ''Dopplerons,'' in saturated absorption spectroscopy. Here, the Doppler shift of a moving atom in an intense standing-wave field induces multiphoton resonances at certain select velocities. This phenomenon was later observed in the context of laser cooling. Another line of work, initiated recently [21,22], showed that an atom (or molecule) can be localized to subwavelength precision based on the conditional detection of fluorescence photons as the atom passes through a standing-wave field. These works hint at the connection between directional interference, absorption spectroscopy, and spatial localization.

We provide an illustrative calculation for the case $N = 2$ shown in Fig. 1. This uses two signal frequencies and two drive frequencies to complete three-photon resonance for each direction. The general case of multiphoton (sinusoidal) interference will be discussed later. While we focus on a multilevel system, we note that Doppleron-type resonances can also be observed in a two-level system, provided the one-photon detunings and field strengths dominate the linewidths in a saturated absorption process [23]. The theory of photoelectron counting has been developed in the semiclassical [24] and quantum field [25] regimes. One begins by calculating a perturbative transition rate of the detector atoms interacting with the field.

In the level scheme of Fig. 1, the intermediate levels c_j are off-resonant by detunings $\Delta_{1\pm} = \omega_{c_1 b} - \nu_\pm$ and $\Delta_{2\pm} = \omega_{ac_2} - \nu_\pm$. Assuming that the signal Rabi frequency Ω_S is the same for the two transitions, the interaction Hamiltonian in the rotating wave approximation ($\Omega_S, \Omega_D \ll \nu_\pm, \omega_0$) is given by

$$H_I = \hbar\Omega_S(|c_1\rangle\langle b|e^{i\Delta_{1\pm}t} + |a\rangle\langle c_2|e^{i\Delta_{2\pm}t} + \text{H.c.}) + \hbar\Omega_D(|c_1\rangle\langle c_2|e^{i(\Delta_{1\pm}+\Delta_{1\pm})t} + \text{H.c.}). \quad (1)$$

The Schrödinger equations for the state amplitudes are next derived. For large one-photon detunings $\Delta_{j\pm} \gg \Omega_S, \Omega_D$, the intermediate levels c_j can be adiabatically eliminated by setting the time derivatives of the slowly varying amplitudes, $\tilde{c}_j = c_j \exp(-i\Delta_{j\pm}t)$, to zero. This furnishes an effective coupling between levels a and b:

$$i\dot{a} - \frac{\Omega_S^2}{\Delta_{2\pm}}a = -\frac{\Omega_S^2\Omega_D}{\Delta_{1\pm}\Delta_{2\pm}}b, \quad (2)$$

and similarly with $a \leftrightarrow b$ and $1 \leftrightarrow 2$. Apart from dispersive phase shifts, the effective coupling is thus described by a three-photon Rabi frequency, $\Omega_{\text{eff}} = (\Omega_S^2\Omega_D)/(\Delta_{1\pm}\Delta_{2\pm})$. In the usual perturbative regime, $1/\Delta_{j\pm} \ll t \ll 1/\Omega_{\text{eff}}$, the rate of excitation from b to a is given to lowest order by a third-order Fermi golden rule:

$$R^{(3)} = 2\pi\left|\frac{\Omega_S^2\Omega_D}{\Delta_{1\pm}\Delta_{2\pm}}\right|^2\delta(\omega_{ab} + \omega_\pm - 2\nu_\pm). \quad (3)$$

This gives the effective rate of two-photon absorption of the signal field $\nu_\pm$ when assisted by the drive field $\omega_\pm$.

The application to subwavelength interference proceeds as follows. As the $\pm$ channels realize distinct resonances, the atoms will absorb two photons from one signal beam or the other, but never one photon from each beam. As a consequence, the spatial period of the fringes will carry the two-photon wavelength, which is one-half the wavelength of each photon, the same as achieved by a quantum, entangled state of the form $|2, 0\rangle + |0, 2\rangle$.

Formally, in Fig. 1, we can write the net electric field as seen by atoms parallel to the surface (x) as consisting of two pairs of counterpropagating signal fields (of same intensity) and the normally incident drive fields:

$$E(x,t) = \mathcal{E}_S[e^{i(k_+x-\nu_+t)} + e^{i(k_-x-\nu_-t)}] + \mathcal{E}_D[e^{-i\omega_+t} + e^{-i\omega_-t}] + \text{c.c.}, \quad (4)$$

where $k_\pm = \pm(\nu_\pm/c)\cos\theta$. Keeping the spatial dependence in view, the third-order excitation rate of the atoms takes the general form

$$R^{(3)}(x,t) \propto \frac{d}{dt}\left|\int_0^t dt_3\int_0^{t_3}dt_2\int_0^{t_2}dt_1\langle a|H_I(x,t_3)H_I(x,t_2)H_I(x,t_1)|b\rangle\right|^2, \quad (5)$$

where the interaction Hamiltonian is given in Eq. (1), with $\Omega_j(x,t) = 2d_j\mathcal{E}_j(x,t)/\hbar$ for each wave. Now, under conditions of three-photon resonance, the leading contributions to the above integral will comprise exactly the two channels for the

frequency-selective excitation shown in Fig. 1, whose rates were calculated in Eq. (3). That is, the only two significant terms in the field product will be those for which the same beam, + or −, contributes twice:

$$R^{(3)}(x,t) \propto \frac{d}{dt}\left| e^{i2k_+x} r_+^{(3)}(t) + e^{i2k_-x} r_-^{(3)}(t) \right|^2; \quad (6)$$

$$r_\pm^{(3)}(t) = \int_0^t dt_3 \int_0^{t_3} dt_2 \int_0^{t_2} dt_1 [\mathcal{E}_S e^{i\Delta_{1\pm}t_1}] \times [\mathcal{E}_D e^{-i(\Delta_{1\pm}+\Delta_{2\pm})t_2}][\mathcal{E}_S e^{i\Delta_{2\pm}t_3}], \quad (7)$$

where the dipole moments have been suppressed. If the one-photon detunings are large, $\Delta_{j\pm} \gg \nu_+ - \nu_-$, then the excitation amplitudes $r_\pm(t)$ are approximately equal, and the single beam, two-photon spatial frequencies $2k_\pm$ make up the interference pattern, i.e., the interbeam cross terms $\exp[i(k_+ + k_-)x]$ are absent because they are out of three-photon resonance.

We can generalize this semiclassical scheme to many photons. We invoke a multiphoton resonance as illustrated in Fig. 2. Each of the two directions of propagation ± is now associated with N distinct frequencies. The signal fields $\nu_{n\pm}$ are absorbed and a single drive field ω_0 is emitted (which is common to both channels). The N signal photons obey a *sum* frequency resonance:

$$\sum_{n=1}^{N} \nu_{n\pm} = \omega_{ab} + (N-1)\omega_0 \equiv N\nu_0, \quad (8)$$

which ensures that, despite the multimode nature of each beam, the N-photon wave vector, $N\nu_0/c = 2\pi/(\lambda_0/N)$, is the same for both beams, providing effectively monochromatic spatial coherence to the fringe pattern. Furthermore, we require that any interchange of photons between beams, $\nu_{n+} \leftrightarrow \nu_{n'-}$, results in a loss of resonance, which identifies the detector bandwidth as the fundamental unit of measure for the frequency steps. For N-photon absorption of the signal, the third-order rate of excitation in Eq. (3) generalizes to (assuming equal detunings for the intermediate levels)

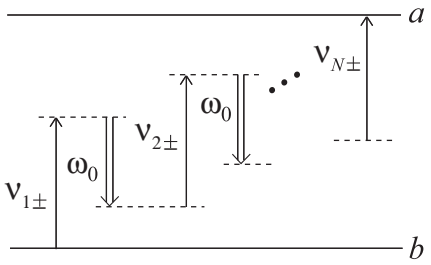

FIG. 2. Multiphoton resonance for two wave vectors $k_\pm$. $2N-1$ photons resonantly excite the atom, with N photons coming from the + (or −) beam. A single drive frequency ω_0 assists the same resonance for both beams, provided the sum frequency of the signal photons is fixed.

$$R^{(2N-1)} = 2\pi \left| \frac{\Omega_S^N \Omega_D^{N-1}}{\Delta_\pm^{2N-2}} \right|^2 \delta(\omega_{ab} + (N-1)\omega_0 - N\nu_0).$$

The analysis proceeds similar to the $N = 2$ case, except that the two-photon bichromatic wave vectors for the beams in Eq. (6) are replaced by the N-photon monochromatic wave vectors $\pm N(\nu_0/c)\cos\theta$.

Hence, two-beam semiclassical lithography exactly simulates quantum field lithography [5] with unlimited spatial coherence. Moreover, the visibility is only limited by the small difference in excitation amplitudes of the two channels in Eq. (7). To achieve frequency-selective multiphoton excitation, the criterion for choosing the frequency separations of the $2N$ signal beams is governed by the bandwidth, namely, that neighboring channels remain distinguishable in the presence of effects such as power broadening and vibrational/collisional linewidths. This qualifies the sense in which the substrate is a "narrow band" detector. However, since sharp (atomic type) resonances are not required, we anticipate that this will be broadly applicable to photoresists.

We now generalize the semiclassical scheme to multiple beams, i.e., diffraction, as shown in Fig. 3 for $N = 2$. Each point on the slit plane is associated with two complementary frequencies, ν_{1k} and ν_{2k}, that satisfy a sum frequency resonance achieved through opposing spatial chirps created using inverted prisms. Then, photon pairs from a single spatial point on the slit plane will be absorbed collinearly (i.e., the same wave vector) in the focal plane. This simulates the multimode state vector $|2,0,\ldots,0\rangle + \cdots + |0,\ldots,0,2\rangle$. As shown for quantum field lithography [6], this would achieve subwavelength

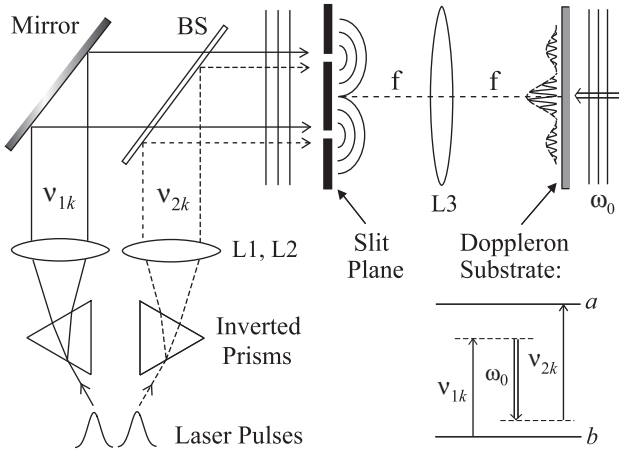

FIG. 3. Subwavelength diffraction for classical light. Two laser pulses are given opposite spatial chirps using inverted prisms, and the resulting beams are combined by a beam splitter (BS) to illuminate the slit plane with a position-dependent frequency doublet, such that $\nu_{1k} + \nu_{2k} = \text{const}$. This creates a correlation between wave vector and frequency pairs in the focal plane of lens L3, and writes a two-photon pattern onto the Doppleron substrate in both carrier and envelope.

resolution not only in the carrier fringe (double-slit interference), but also in the envelope (single slit diffraction). The ratio of the pulse bandwidth to detector bandwidth determines the effective number of wave vectors constituting the diffraction pattern, or equivalently, the number of discrete partitions of the slit apertures.

We note that the above semiclassical approach can be adapted to imaging, for example, two lenses in an f-f-f-f configuration. Here, one introduces a correlation between wave vector and frequency in the focal plane of the first lens *after* the light has passed through the object, i.e., once the angular spectrum of the light is prescribed by the diffracting apertures. This can be accomplished by using a filter array in the focal plane that selects the desired spatial chirp from a broadband input. Using a dual filter array, one can associate a frequency pair (ν_{1k}, ν_{2k}) with each wave vector such that the sum frequency is fixed: $\nu_{1k} + \nu_{2k} = \text{const}$. The result is a subdiffraction image spot (airy disk) created on the substrate in the image plane when vignetting due to the lens apertures is taken into account. As in the diffraction scheme, the bandwidth of the multiphoton process effectively discretizes the angular spectrum on the substrate, which in turn determines the resolution needed for the filter array in this imaging scheme.

In practice, one could also use a Raman-type multiphoton process where ν_{1k} is absorbed and ν_{2k} is emitted, such that the *difference* frequency is constant. No drive field would be required in this case, lowering the excitation order. In general, Raman vibrational transitions have lifetimes on the order of 1 ps, which generally increases as temperature is decreased, where we note that liquid nitrogen temperatures are often used in semiconductor processing. However, even at room temperature, vibrational lifetimes as long as 0.5 ns [26] (300 MHz) have been observed in organic films. Similarly narrow linewidths have also been observed for Raman-excited spin transitions in a solid at room temperature [27]. Finally, we note that new resists have been developed for matter-wave lithography with laser cooled alkali atoms [28]. These laser cooled atoms generally exhibit ultranarrow optical and Raman linewidths below 10 MHz. This narrow linewidth would permit high-order Raman-based lithography.

In conclusion, we have shown how to achieve subwavelength diffraction and imaging with classical light, with high efficiency, visibility, and spatial coherence. We reiterate the basic point that a directionally selective, narrow band detection process allows classical laser light to resemble a quantized entangled field exhibiting path-number correlations, emphasizing the role of measurement in defining the interferometric properties of light.

The authors thank the support of AFRL, AFOSR, DARPA-QuIST, TAMU TITF initiative, ONR, and the Robert A. Welch Foundation (Grant No. A-1261).

[1] J. W. Strutt, Philos. Mag. **47**, 81 (1874); Philos. Mag. **8**, 261 (1879).
[2] M. O. Scully and K. Drühl, Phys. Rev. A **25**, 2208 (1982).
[3] M. O. Scully, *Conference on Effects of Atomic Coherence and Interference in Quantum Optics, Crested Butte, Colorado, 1993* (unpublished).
[4] A. Muthukrishnan, M. O. Scully, and M. S. Zubairy, J. Opt. B **6**, S575 (2004).
[5] A. N. Boto, P. Kok, D. S. Abrams, S. L. Braunstein, C. P. Williams, and J. P. Dowling, Phys. Rev. Lett. **85**, 2733 (2000).
[6] M. D' Angelo, M. V. Chekhova, and Y. Shih, Phys. Rev. Lett. **87**, 013602 (2001).
[7] G. S. Agarwal and M. O. Scully, Opt. Lett. **28**, 462 (2003).
[8] U. W. Rathe and M. O. Scully, Lett. Math. Phys. **34**, 297 (1995).
[9] S. J. Bentley and R. W. Boyd, Opt. Express **12**, 5735 (2004).
[10] A. Pe'er, B. Dayan, M. Vucelja, Y. Silverberg, and A. A. Friesem, Opt. Express **12**, 6600 (2004).
[11] K. Wang and D.-Z. Cao, Phys. Rev. A **70**, 041801(R) (2004).
[12] M. Göppert-Mayer, Ann. Phys. (Leipzig) **9**, 273 (1931).
[13] R. Hanbury-Brown and R. Q. Twiss, Proc. R. Soc. A **242**, 300 (1957).
[14] R. J. Glauber, Phys. Rev. **130**, 2529 (1963); also see *Quantum Optics*, edited by S. M. Kay and A. Maitland (Academic, London, 1970), p. 53.
[15] B. R. Mollow, Phys. Rev. **175**, 1555 (1968).
[16] H. J. Kimble and L. Mandel, Phys. Rev. A **30**, 844 (1984), and references therein.
[17] S. Haroche and F. Hartmann, Phys. Rev. A **6**, 1280 (1972).
[18] E. Kyrola and S. Stenholm, Opt. Commun. **22**, 123 (1977).
[19] P. R. Berman and J. Ziegler, Phys. Rev. A **15**, 2042 (1977).
[20] J. Reid and T. Oka, Phys. Rev. Lett. **38**, 67 (1977); S. M. Freund, M. Römheld, and T. Oka, Phys. Rev. Lett. **35**, 1497 (1975); N. P. Bigelow and M. G. Prentiss, Phys. Rev. Lett. **65**, 555 (1990); J. J. Tollett *et al.*, Phys. Rev. Lett. **65**, 559 (1990).
[21] A. M. Herkommer, W. P. Schleich, and M. S. Zubairy, J. Mod. Opt. **44**, 2507 (1997).
[22] S. Qamar, S.-Y. Zhu, and M. S. Zubairy, Phys. Rev. A **61**, 063806 (2000).
[23] D. E. Pritchard and P. L. Gould, J. Opt. Soc. Am. B **2**, 1799 (1985).
[24] L. Mandel, E. C. G. Sudarshan, and E. Wolf, Proc. Phys. Soc. London **84**, 435 (1964).
[25] M. O. Scully and W. E. Lamb, Phys. Rev. **179**, 368 (1969).
[26] A. Xie, L. Van der Meer, and R. H. Austin, J. Biol. Phys. **28**, 147 (2002).
[27] R. Kolesov, Phys. Rev. A **72**, 051801(R) (2005).
[28] J. H. Thywissen, K. S. Johnson, R. Younkin, N. H. Dekker, K. K. Berggren, A. P. Chu, and M. G. Prentiss, J. Vac. Sci. Technol. B **15**, 2093 (1997).